



Microstructure-property relations in WC-Co coatings sprayed from combinatorial Ni-plated and nanostructured powders

J.-C. Han^{a,1}, M. Jafari^{a,1}, C.-G. Park^{a,b,*}, Jae-Bok Seol^{b,**}

^a Department of Materials Science and Engineering, POSTECH, 790-784 Pohang, South Korea

^b National Institute for Nanomaterials Technology (NINT), POSTECH, 790-784 Pohang, South Korea

ARTICLE INFO

Keywords:

WC-Co coating
HVOF thermal spray
Decarburization
Microstructure
Mechanical properties

ABSTRACT

In this study, we addressed the effects of Ni-plating and nanostructuring of WC-Co powders on the microstructure-property relations and WC decarburization of WC-Co composite coatings. By high velocity oxygen fuel (HVOF) spraying, the coating materials were produced from four different powders, referred to as microstructured WC-Co (mc-WC), nanostructured WC-Co (nc-WC), Ni-plated microstructured WC-Co (Ni/mc-WC) and Ni-plated nanostructured WC-Co (Ni/nc-WC). We found that the coatings, deposited from Ni-free powders, undergo a high level of decarburization, thereby yielding W₂C phase formation in brittle amorphous W-rich Co matrix that could be preferential site for crack propagation. On the contrary, the Ni-plating treatment could reduce the amount of decarburization of the coatings, resulting in the uniform distribution of WC phase in the W-depleted Co matrix. Consequently, we revealed the underlying mechanisms responsible for WC decarburization in the coatings, and further suggested that the coating deposited from Ni-plated and nanostructured powders exhibits a superior combination of hardness and fracture toughness as compared to other coatings.

1. Introduction

WC-Co ceramic-metal (cermet) composites containing over 70 vol% WC particles within Co matrix have been widely applied as cutting, drilling, machining tools, extrusion dies and etc. [1–4]. In addition, thermally sprayed WC-Co coatings have been gratified for the demands on protecting different substrates against wear, e.g. seat and gate components in petroleum industry, bridle-rolls and pinch-rolls in hot rolling of steels, landing gear of aircrafts, etc. [4–11].

The common techniques to produce WC-Co coatings include air plasma spraying (APS), high-velocity oxygen-fuel (HVOF) spraying and detonation spray coating (DSC). Compared to the coatings deposited by APS and DSC techniques, HVOF spraying provides higher velocity and lower temperature for in-flight particles and produces more compacted WC-Co coatings containing a larger fraction of retained WC phase [9–11]. From a technological point of view, desired microstructure of WC-Co coatings contains WC particles uniformly dispersed in the metallic Co matrix, to provide attractive combination of hardness, fracture toughness and wear resistance. However, the major technological bottleneck in HVOF-sprayed WC-Co coatings lies in controlling the extent of WC decarburization during coating deposition, which leads to

the formation of non-WC phases such as W₂C, metallic W, and nanocrystalline Co-W-C phases. In general, non-WC phases deteriorate the fracture toughness and wear resistance of the coatings due to their brittleness [11–14]. Therefore, preventing the formation of non-WC phases and understanding of the underlying phase transformations during HVOF spraying are still challenging issues needing further investigations.

As followed by previous interpretations responsible for decarburization mechanisms [14–16], when WC-Co particles are exposed to high temperature HVOF flame (~3000 °C), Co matrix melts upon which WC grains begin to be dissolved into the liquid Co. The oxidizing atmosphere of HVOF flame causes a part of dissolved carbon to be oxidized in the form of CO/CO₂ gas mixture leading to decarburization. Subsequently, precipitation of W₂C from W-rich Co matrix takes place during solidification upon impact to the substrate. Another explanation for W₂C formation during HVOF spraying includes direct oxidation of WC located at the surface of feedstock powder due to their exposure to oxidizing environment of HVOF flame [15].

Numerous strategies implemented to reduce decarburization level during HVOF spraying of WC-Co powder can be classified into two categories. First, optimization of spray conditions by using high velocity

* Correspondence to: C.-G. Park, Department of Materials Science and Engineering, POSTECH, 790-784 Pohang, South Korea.

** Corresponding author.

E-mail addresses: cgpark@postech.ac.kr (C.-G. Park), jb_seol@postech.ac.kr (J.-B. Seol).

¹ Authors equally contributed to this paper.

air fuel (HVOF) with lower flame temperature instead of HVOF [17], utilizing combustion flame with reducing atmosphere [18], improving the spray parameters such as fuel/oxygen ratio and in-flight particles velocity [19], and using a shroud to introduce an inert gas into the HVOF spraying environment [20]. Second, tailoring the chemical composition of WC-Co powder by addition of 0.5–1.2% graphite to initial powder in order to compensate the carbon loss occurs during HVOF process [21], and incorporating solid lubricants such as Cu, MoS₂, BaF₂ and CaF₂ to initial WC-Co powder [22].

Profound progress in reducing WC decarburization has been achieved through development of metal-clad WC-Co powder. In this regard, Baik et al. [23] developed a thin Co layer around WC-Co powder particles by immersing them into Co-hydrate sol and hydrogen reduction. According to their results, the coating deposited from Co-coated powder experienced lower decarburization during HVOF and exhibited higher wear resistance compared to the conventional WC-Co coating. Mateen et al. [11] and Saha & Khan [24] reported that decarburization can be suppressed by using Co-coated WC-Co powder produced via chemical vapor deposition (CVD); however, W₂C was still detected in the phase composition of the coating. More recent work by Jafari et al. [1] suggested that utilizing Ni-plated WC-Co powder prevents decarburization to a larger extent leading to the enhanced mechanical properties for WC-Co coatings.

It is well established that decarburization becomes more pronounced for nanostructured WC-Co coating due to the higher surface-to-volume ratio of nano-sized WC, which stimulates its dissolution into the liquid Co [8,25,26]. This leads to an inferior wear resistance for nanostructured coatings as compared to conventional microstructured ones; however, the explanations about the effects of nanostructured WC-Co powder on properties of HVOF coatings have been controversial to date. In addition, there has been a lack of comprehensive study to investigate the combined effects of Ni-plated and nanostructured WC-Co powder on microstructure and properties of the coatings.

In this study, detailed WC decarburization mechanisms of micro- and nano-structured WC-Co coatings were investigated by advanced characterization techniques including scanning transmission electron microscopy (STEM) equipped with high angle annular dark field (HAADF) and energy dispersive spectrometer (EDS). A special emphasis was placed on the microstructural evolution and the related mechanical properties of different Co matrices (crystalline W-depleted Co matrix and amorphous W-rich Co matrix) in terms of their hardness and elastic modulus examined by using nano-indentation experiments. Lastly, electroless Ni plating was executed to develop a dense and uniform Ni layer around individual micro- and nano-structured WC-Co powder particles. The role of electroless Ni layer on protecting the internal micro- and nano-structured WC-Co powder particles against severe WC dissolution and decarburization has been discussed in detail.

2. Experimental procedure

2.1. Feedstock powders and coating preparation

Commercial microstructured WC-12Co (mc-WC) (provided by Metallization Ltd.), nanostructured WC-12Co (nc-WC), electroless Ni-plated microstructured WC-12Co (Ni/mc-WC) and electroless Ni-plated nanostructured WC-12Co (Ni/nc-WC) powders were used as the starting materials. Fig. 1 shows the overall sequences of experimental procedure. Details of preparation methods for nc-WC, Ni/mc-WC and Ni/nc-WC powders can be found in the previous studies by the authors [1,27].

Electroless Ni-plating process resulted in the development of dense and uniform Ni layers with thickness of ~0.5–1.5 μm for Ni/mc-WC and < 100 nm for Ni/nc-WC powders (Supplementary information, Fig. S1). General characteristics of the powders in terms of chemical composition, WC-Co particle size and WC size are given in Table 1.

The four types of feedstock powders were deposited onto ST-37 steel

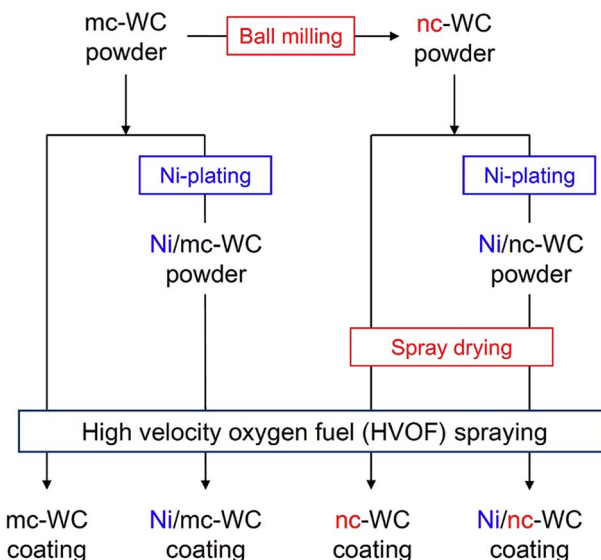


Fig. 1. A flowchart representing the overall sequences of experimental procedure.

Table 1
Chemical composition, WC-Co particle size and WC size of different powders.

Powder	Chemical composition (wt%)					Particle size (μm)	Carbide size
	W	C	Co	Ni	Others		
mc-WC	Balance	5.3	12.1	–	0.8	15–45	1–6 μm
Ni/mc-WC	Balance	5.1	11.7	5.5	1.2	15–45	1–6 μm
nc-WC	Balance	5.3	11.8	–	1.1	5–50	5–30 nm
Ni/nc-WC	Balance	5.3	11.4	3.4	1.3	5–45	5–30 nm

substrates with dimension of Ø30 × 5 mm using an HVOF spray system (MET JET III HVOF torch, Metallization Ltd) with parameters given in ref. [27]. Thickness and surface roughness of as-sprayed coatings were measured by Elcometer coating thickness gauge and Taylor-Hobson roughness tester.

2.2. Microstructure characterization of powders and coatings

X-ray diffractometry (XRD) (Philips diffractometer, 40 kV, Cu(Kα) = 0.15406 nm, step size: 0.05°/1 s) was performed to determine the phase composition of the powders and coatings. The recorded XRD patterns were characterized by PANalytical X'Pert High Score software and the average phase fractions were determined using XRD data sets for each sample. An elemental analysis tool (Elementar Vario EL III, Germany) was used to measure the C content of the powders and coatings in order to determine the exact amount of decarburization. High-resolution field-emission scanning electron microscopy (FE-SEM) (JEOL JSM-7401F) was utilized to examine the general microstructure and phase distribution in the powders and coatings. In addition, the porosity of the coatings was measured through cross-sectional SEM images analysis using Clemex software. To distinguish WC and W₂C phases in the coatings microstructure, back-scattered electron (BSE) mode of SEM in conjunction with electron backscatter diffraction (EBSD) analysis, installed on a dual-beam focused ion beam (FIB, FEI Nano-Lab 600), was utilized. The EBSD analyses were conducted at an accelerating voltage of 20 kV, incident beam current of 22 nA and step size of 20 nm. The acquired data were post-processed using the TSLs OIM 5.0 software. A confidence index (CI) of 0.20 was selected for phase identification. Particular regions of the coatings microstructure were characterized by transmission electron microscopy (TEM) (JEOL 2100F TEM), operated at an accelerating voltage of 200 kV, and the corresponding selected area diffraction pattern (SADP). TEM samples from the coatings were prepared by lift-out method using FIB techni-

Download English Version:

<https://daneshyari.com/en/article/5454862>

Download Persian Version:

<https://daneshyari.com/article/5454862>

[Daneshyari.com](https://daneshyari.com)